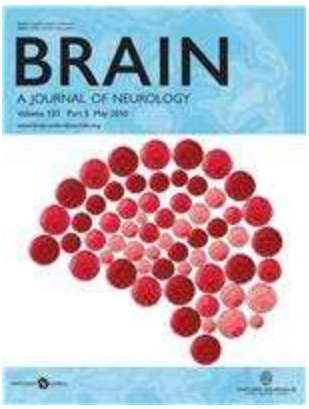

Gait-related cerebral alterations in Parkinson patients with freezing of gait

Journal:	*Brain*
Manuscript ID:	BRAIN-2010-00592.R2
Manuscript Type:	Original Paper
Date Submitted by the	12-Sep-2010

Complete List of Authors:	Snijders, Anke; Radboud University Nijmegen Medical Centre, Donders Institute for Brain, Cognition and Behaviour, Department of Neurology; Radboud University Nijmegen, Donders Institute for Brain, Cognition and Behaviour, Centre for Cognitive Neuroimaging Leunissen, Inge; Radboud University Nijmegen Medical Centre, Donders Institute for Brain, Cognition and Behaviour, Department of Neurology; Radboud University Nijmegen, Donders Institute for Brain, Cognition and Behaviour, Centre for Cognitive Neuroimaging Bakker, Maaike; Radboud University Nijmegen Medical Centre, Donders Institute for Brain, Cognition and Behaviour, Department of Neurology; Radboud University Nijmegen, Donders Institute for Brain, Cognition and Behaviour, Centre for Cognitive Neuroimaging Overeem, Sebastiaan; Radboud University Nijmegen Medical Centre, Donders Institute for Brain, Cognition and Behaviour, Department of Neurology Helmich, Rick; Radboud University Nijmegen Medical Centre, Donders Institute for Brain, Cognition and Behaviour, Department of Neurology; Radboud University Nijmegen, Donders Institute for Brain, Cognition and Behaviour, Centre for Cognitive Neuroimaging Bloem, Bastiaan; Radboud University Nijmegen Medical Centre, Donders Institute for Brain, Cognition and Behaviour, Department of Neurology Toni, Ivan; Radboud University Nijmegen, Donders Institute for Brain, Cognition and Behaviour, Centre for Cognitive Neuroimaging; Radboud University Nijmegen, Donders Institute for Brain, Cognition and Behaviour, Centre for Cognition
Key Words:	
Please choose up to 5 keywords from the list:	Parkinsons disease, motor planning, gait, pedunculopontine nucleus

Gait-related cerebral alterations in Parkinson patients with freezing of gait

Anke H Snijders[1,2], Inge Leunissen[1,2], Maaike Bakker[1,2], Sebastiaan Overeem[2], Rick C. Helmich[1,2], Bastiaan R. Bloem[2], Ivan Toni[1,3]

Radboud University Nijmegen , Donders Institute for Brain, Cognition and Behaviour: [1]Centre for Cognitive Neuroimaging, [3]Centre for Cognition, The Netherlands

Radboud University Nijmegen Medical Centre, Donders Institute for Brain, Cognition and Behaviour: [2]Department of Neurology, The Netherlands

Corresponding Author:

Prof. Bastiaan R. Bloem

Department of Neurology, 935

Radboud University Nijmegen Medical Centre

PO Box 9101, 6500 HB Nijmegen

The Netherlands

Tel: 00-31-24-3615202

Email: B.Bloem@neuro.umcn.nl

Words: 5771

Abstract (324 words)

Freezing of gait is a common, debilitating feature of Parkinson's disease. We have studied gait planning in patients with freezing of gait, using motor imagery of walking in combination with fMRI. This approach exploits the large neural overlap that exists between planning and imagining a movement. In addition, it avoids the confounds introduced by brain responses to altered motor performance and somatosensory feedback during actual freezing episodes.

We included 24 patients with Parkinson's disease [12 patients with freezing of gait ('freezers'), 12 matched patients without freezing of gait ('non-freezers')] and 21 matched healthy controls. Subjects performed two previously validated tasks: motor imagery of gait, and a visual imagery control task. During fMRI scanning, we quantified imagery performance by measuring the time required to imagine walking on paths of different width and length. In addition, we used voxel-based morphometry to test whether between-group differences in imagery-related activity were related to structural differences.

Imagery times indicated that freezers, non-freezers, and controls engaged in motor imagery of gait, with matched task performance. During motor imagery of gait, freezers showed more activity than non-freezers in the mesencephalic locomotor region. Freezers also tended to have decreased responses in mesial frontal and posterior parietal regions. Furthermore, freezers had grey matter atrophy in a small portion of the mesencephalic locomotor region. The gait-related hyperactivity of the mesencephalic locomotor region correlated with clinical parameters (freezing of gait severity and disease duration), but not with the degree of atrophy.

These results indicate that Parkinson's disease patients with freezing of gait have structural and functional alterations in the mesencephalic locomotor region. We suggest that freezing of gait might emerge when altered cortical control of gait is combined with a limited ability of the mesencephalic locomotor region to react to that alteration. These limitations might become particularly evident during challenging events that require precise regulation of step length and gait timing, such as turning or initiating walking, which are known triggers for freezing of gait.

INTRODUCTION

Freezing of gait (FOG) is an episodic gait disorder during which the feet appear 'glued to the floor' (Bloem *et al.,* 2004). The pathophysiology underlying FOG remains largely unknown. Behavioural studies have identified several gait alterations in PD patients with FOG ("freezers"), even when the patient is not experiencing an actual FOG episode. Alterations include premature timing of muscle activations (Nieuwboer *et al.,* 2004), increased variability of gait (Hausdorff *et al.,* 2003), increased temporal gait asymmetry (Plotnik *et al.,* 2008), and faulty generation of postural adjustments before step initiation (Jacobs *et al.,* 2009a). A recent paper suggested that FOG may be caused by a failure to generate adequate amplitudes for the intended movement. This will lead to a progressive reduction of step size that may culminate into a FOG event (Chee *et al.,* 2009). This so-called sequence effect could result from defective stride length amplitude setting by the supplementary motor area (SMA) and its maintenance by the basal ganglia, leading to a mismatch between intention and automation (Chee *et al.,* 2009). However, empirical tests of this hypothesis are difficult, because most non-invasive neuroimaging methods are not suitable for assessing gait (Bakker *et al.,* 2007b).

Some experimental approaches can bypass these difficulties, allowing researchers to study the cerebral correlates of FOG (Bartels *et al.,* 2006; Fabre *et al.,* 1998; la Fougere *et al.,* 2009; Matsui *et al.,* 2005). One possibility is to focus on the planning phase of walking movements, rather than the manifestation of actual FOG episodes. Motor imagery (asking subjects to imagine a particular movement) exploits the large functional and neural overlap between motor planning and motor imagery of a movement (Cisek and Kalaska, 2004; Jeannerod, 1994; Miller *et al.,* 2010). Imagining a movement is sensitive to motor control variables (Gentili *et al.,* 2004), it is contingent on the current physical configuration of the subject (Nico *et al.,* 2004; de Lange *et al.,* 2006), and it relies on neural processes similar to those evoked during performance and planning of the same movement (Stephan *et al.,* 1995; la Fougere *et al.,* 2009). We have recently shown that motor imagery of gait follows similar motor constraints as actual walking (Bakker *et al.,* 2007a). Accordingly, motor imagery of gait has been used repeatedly to study human walking using fMRI (Bakker *et al.,* 2008; la Fougere *et al.,* 2009) or PET (Malouin *et al.,* 2003).

Although motor imagery of gait is likely to engage only a portion of the cerebral circuits controlling walking, it has several advantages for investigating FOG. First, motor imagery provides opportunities for studying alterations in the planning of gait, which may be a crucial element in FOG pathophysiology (Chee *et al.,* 2009; Jacobs *et al.,* 2009b). Second, meaningful cerebral comparisons between patients and controls

require matched behavioural performance (Price and Friston, 2002). This condition can be met with motor imagery of gait, whereas real motor performance will often differ between patients and controls. Third, motor imagery of gait allows us to isolate cerebral responses related to walking, distinct from alterations in motor performance and somatosensory feedback produced by actual FOG episodes (Almeida *et al.,* 2005).

Accordingly, we used motor imagery of gait in combination with fMRI to study the cerebral correlates of gait planning in patients with and without FOG. Stimulated by current hypotheses concerning FOG pathophysiology – which mainly deal with deficits in regulating step length and gait timing (Chee *et al.,* 2009; Plotnik *et al.,* 2008) – we also included a behavioural control experiment where actual gait was electrophysiologically quantified. Finally, we used voxel-based morphometry to assess whether between-group differences in imagery-related activity were related to structural differences.

METHODS

Subjects

We included 25 patients with PD, 13 freezers and 12 non-freezers who were matched for disease severity and duration (Table 1 – one freezer was excluded from the analyses due to his inability to engage in imagery, see below). Patients were diagnosed according to the UK Brain Bank criteria (Hughes *et al.,* 1992). All patients except one used dopaminergic medication (levodopa or dopamine-agonists). Patients were examined in the morning, at least 12 hours after intake of the last dose of antiparkinson medication. Disease severity was assessed using the Hoehn & Yahr stages and Unified Parkinson's Disease Rating Scale (UPDRS). Patients with marked resting tremor were excluded. In the remaining patients, we carefully controlled for tremor influences on scanning results by recording electromyography (see below). Twenty-one healthy volunteers, matched for age and gender, served as controls (Table 1).

Freezers were identified based on three criteria: (1) convincing subjective reports of FOG, based on consistent and characteristic accounts of the phenomenon (including the typical feeling of the feet being glued to the floor); (2) patient's recognition of typical phenotype when this was demonstrated to them by an experienced clinician, or using the New Freezing of Gait Questionnaire (NFOG-Q) video (Nieuwboer *et al.,* 2009). In addition, a standardized and videotaped gait trajectory was performed containing specific elements known to provoke FOG (Snijders *et al.,* 2008). These videos were rated off-line for the presence of FOG by two different experts. Nine of the 12 freezers (75%) also showed FOG during physical examination. None of

the non-freezers experienced subjective freezing, recognized the phenotype when this was demonstrated to them, or manifested freezing during physical examination. The median NFOG-Q score (Nieuwboer *et al.,* 2009) for freezers was 12.4, range 5-27. The score for non-freezers was 0.

All subjects were right-handed according to the Edinburg Handedness Inventory, had no cognitive dysfunction (Mini-Mental State Examination >24, Frontal Assessment Battery >13), and no vestibular, orthopaedic, neurological or psychiatric diseases. Before participation, subjects received the (unrevised) Vividness of Motor Imagery Questionnaire (VIMQ) (Isaac *et al.,* 1986) to screen for ability to perform motor imagery. When a subject was unable to perform motor imagery (VIMQ score >200), the subject was excluded (one freezer with a score of 240). Patients and controls were equally able to perform motor imagery (one-way ANOVA, effect of group: $F(2,41) = 1.4$, $p = 0.24$), with scores comparable to age-matched healthy subjects (Mulder *et al.,* 2007). The study was approved by the local ethics committee, and written informed consent was obtained from all subjects prior to the experiment according to the Declaration of Helsinki.

Tasks

We used a behaviourally validated protocol (Bakker *et al.,* 2007a) used in a previous fMRI study in young healthy subjects (Bakker *et al.,* 2008). Briefly, subjects performed two tasks: motor imagery of gait (MI), during which they had to imagine walking along a path, and a matched visual imagery control task (VI), during which they imagined seeing a disc moving along the path (Figure 1). Subjects were presented with a picture of a path with a target placed on it. They were asked to either imagine themselves walking towards the target (MI), or to imagine a disc moving towards the target. During both tasks, the motion-relevant portion of the path could have two different widths (narrow, broad) and five different distances (2, 4, 6, 8, and 10 m). These manipulations allowed us to monitor the subject's ability to perform motor imagery in the scanner (Bakker *et al.,* 2008). Specifically, imagery times for both VI and MI should vary with alterations in path length. Furthermore, only MI times should be susceptible to path width alterations, because a narrow path requires precision gait. Conversely, the VI task (a moving disc) should not be influenced by path width (Bakker *et al.,* 2008). The MI and VI tasks were performed in two successive sessions of 25 minutes each, separated by a break outside the scanner. The order of the sessions was counterbalanced across subjects. To control for actual movements related to tremor or overt leg movements, muscle activity from the forearm and lower leg was measured during the fMRI experiment. For further details, see the supplementary material.

After the imagery sessions, we tested subjects' actual walking along the same paths as displayed during the imagery session. Performance on each of the 10 experimental conditions (2 different path widths over 5 different distances) was sampled once, recording the actual walking time with a stopwatch. These measurements served to confirm the relationship between imagined and actual walking performance (Bakker *et al.,* 2007a).

Behavioural analysis

We objectively monitored task performance by testing whether imagery times were modulated by the width and length of the path presented to the subjects. For each trial, imagery time was defined as the time between the button presses indicating the onset and offset of imagery. Trials in which subjects failed to press the button (either at the onset or offset of the imagery phase) were excluded from analyses (freezers mean [range]: 1.1 [0 to 4] trials; non-freezers: 0.5 [0 to 3] trials; controls: 0.5 [0 to 5] trials). Afterwards, the standard deviation (SD) of the mean picture inspection duration and imagery time was computed. Trials outside the mean ± 3 SD range were considered outliers and removed (freezers mean [range]: 1.2 [0 to 3] trials; non-freezers: 0.6 [0 to 2] trials; controls: 0.8 [0 to 2] trials).

We considered the effect of "Group" (analysis 1: patients versus controls; analysis 2: freezers versus non-freezers), "Task" (MI, VI), "Path Width" (narrow, broad) and "Path Length" (2, 4, 6,8,10 m) on imagery time. The significance of the experimental factors was tested within the framework of the General Linear Model using two 2x2x2x5 mixed-effects ANOVAs. When interactions were significant, the simple main effects were investigated by additional ANOVA's. The alpha-level of all behavioural analyses was set at $p<0.05$. In a separate analysis, we used Spearman's correlation to assess the relationship between actual walking times and mean imagery times across the different experimental conditions for patients and controls.

Pre-processing of imaging data

Functional data were pre-processed and analyzed with SPM5 (Statistical Parametric Mapping, www.fil.ion.ucl.ac.uk/spm). Details on MR images pre-processing can be found in the supplementary material.

Statistical analysis of imaging data – first level

The ensuing pre-processed fMRI time series were analyzed on a subject-by-subject basis using an event-related approach in the context of the General Linear Model (Friston *et al.,* 1995). The model was aimed at finding regions in which the cerebral response changed as a function of "Task" (MI, VI) and/or "Path Width". "Path Length" was also considered in the analysis, which gave rise to a model with twenty different regressors of interest. The model also included separate regressors of no interest, modelling BOLD activity evoked by picture inspection, button presses, and incorrect trials, separately for each session. Further details can be found in the supplementary material.

Statistical analysis of imaging data – second level

We report the results of a random effects analysis. The statistical significance of the estimated evoked haemodynamic response was assessed using t-statistics in the context of the General Linear Model. For each subject, four contrast images (MI-broad, MI-narrow, VI-broad and VI-narrow) were calculated and entered into a second level random effects analysis. Analogously to the analysis of the behavioural data, we considered two analyses: Analysis 1 compared controls (c) with patients (p); analysis 2 compared freezers (f) with non-freezers (nf).

First, we identified the cerebral correlates of motor imagery of gait within each group, searching for brain responses that were larger for MI than for VI [analysis 1: cMI>cVI, pMI>pVI; analysis 2: nfMI>nfVI, fMI>fVI]. Second, we identified regions where task-related activity differed between groups, assessing the "Group*Task" interaction [analysis 1: (cMI>cVI) > (pMI>pVI), (pMI>pVI) > (cMI>cVI); analysis 2: (fMI>fVI) > (nfMI>nfVI) , (nfMI>nfVI) > (fMI>fVI)]. Third, we looked for the shared effects (across groups) of environmental constraints (i.e. "Path Width") on MI-related activity, searching for brain responses that were larger during imagined walking on a narrow path than during imagined walking on a broad path [analysis 1: cMI-narrow>cMI-broad, pMI-narrow>pMI-broad; analysis 2: nfMI-narrow>nfMI-broad, fMI-narrow>fMI-broad]. Fourth, we assessed differential effects of "Path Width" between groups, looking at the "Group*Path Width" interaction.

Statistical inference ($p<0.05$) was performed at the cluster-level, correcting for multiple comparisons over the search volume (i.e. the whole brain) using family-wise error, given an intensity threshold of $t> 3.4$ (Friston *et al.,* 1996).

Region of interest analysis

Besides whole brain analyses, statistical inference was also performed on regions of interest that were based on our previous study in healthy controls (Bakker *et al.,* 2008) (see supplementary material for nomenclature and stereotactic coordinates of ROIs). More precisely, we considered the local maxima of the clusters that were previously found to be significantly activated in the following contrasts: 1) "MI>VI" for the analyses considering the effects of "Task" and "Group" described above; and 2) "MI-narrow>MI-broad" for the analyses considering the effects of "Path Width" and "Group". More specifically, we drew spherical ROIs centred at these coordinates with a radius of 8 mm. Statistical inference was performed at the voxel-level, with a family-wise error correction for multiple comparisons ($p<0.05$).

Gait assessment

In a separate behavioural experiment, gait characteristics were measured with an electronic pressure-sensitive walkway (GAITRite, CIR Systems Inc, USA). This system consists of a 4.6 m long walkway, containing six sensor pads encapsulated in a roll-up carpet to produce an active area 61 cm wide and 366 cm long. This system captures the geometry and relative arrangement of each footfall as a function of time, and can detect gait alterations that are typical for PD (Almeida *et al.,* 2005). Subjects were asked to walk at their normal speed. This procedure was repeated three times. We compared normalized step length (step length/leg length) and gait asymmetry (natural logarithm (LN) of the difference in the swing time of the slowest and swing time of fastest foot) between freezers, non-freezers and controls using univariate ANOVA and post-hoc independent sample t-tests.

Brain-disease, brain-behaviour, and structural-functional relationships

We tested whether the activity related to motor imagery of gait was correlated with clinical characteristics (disease severity, disease duration, and freezing severity). We considered the significant between-groups effects obtained in the second level analysis of the imaging data, and correlated subject-specific beta values (relative to the contrast motor imagery minus visual imagery) with the UPDRS score, disease duration, and NFOG-Q score, using Pearson's correlation with an alpha-level set at $p<0.05$. We took part 2 of the NFOG-Q score, looking at severity of FOG.

We also examined whether the activity in motor-imagery related areas was correlated to the kinematic characteristics of gait movements, and whether this effect was different between the three groups. We only considered effects that were robust to the removal of potential outliers (Z-score above/below 2.5 units). We considered the significant between-groups effects obtained in the second level analysis of the imaging data, and we used a generalized linear model with subject-specific beta values (relative to the contrast motor imagery minus visual imagery) as a dependent variable, fixed factor of 'group' and the gait parameters as covariates. The generalized linear model uses the Wald statistic with chi-square distribution, to be able to compute the individual contribution of predictors (Field, 2009). If a significant effect ($p<0.05$) was found, post hoc univariate ANOVA was performed on the different groups with the gait parameter as a covariate.

In addition, we evaluated whether the between-group differences in imagery-related activity was associated with structural differences, performing a voxel-based morphometry analysis (Ashburner and Friston, 2000). We tested whether there were between-groups differences in grey matter, white matter, or cerebral spinal fluid volume (CSF) (analysis 1: Controls versus patients; analysis 2: Freezers versus non-freezers). We assessed regional differences, as well as differences over a regions of interest based on the results of the whole brain fMRI analyses (mesencephalic locomotor region, Table 3), testing for the relevance of structural differences by correlating them to the magnitude of the functional differences (i.e., beta weigths for the MI vs VI contrast). Statistical inference was performed at the voxel level, with a family-wise error correction for multiple comparisons ($p<0.05$). For further details on the voxel-based morphometry analysis, see the supplementary material.

Anatomical inference

Anatomical details of significant signal changes were obtained by superimposing the statistical parametric maps (SPMs) on the anatomical sections of a representative subject of the MNI series. The atlas of Duvernoy was used to identify relevant anatomical landmarks (Duvernoy *et al.,* 1991). The SPM Anatomy Toolbox was used for regions where cytoarchitectonic maps were available (Eickhoff *et al.,* 2005; Scheperjans *et al.,* 2008). We used the WFU PickAtlas Toolversion 2.4 to translate MNI into Talairach coordinates (where necessary for relating our findings to existing literature). To define coordinates of mesencephalic locomotor regions, we used maps and coordinates (Zrinzo *et al.,* 2008; Keren *et al.,* 2009; Eippert *et al.,* 2009). The functional labelling of premotor cortical areas was based on (Mayka *et al.,* 2006) and (Picard and Strick, 1996).

RESULTS

During electrophysiological gait testing patients had a smaller step length and an increased temporal gait asymmetry compared to controls (Table 2).

Behavioural results

Imagery times are shown in Figure 2; statistical values in Table 3**.** During the motor imagery experiment, none of the freezers experienced 'imagined' FOG. Although non-freezers were numerically slower than freezers (and controls) across both imagery tasks, imagery times for VI and MI were not statistically different between groups (no effect of "Group", Table 3, Figure 2). In addition, there was no difference between MI and VI (no effect of "Task", Table 3). The effect of task on imagery times did not differ between groups (no "Task*Group" interaction, Table 3, figure 2B) and showed that all groups performed the imagery adequately. First, there was an effect of increasing path length in both tasks, and this effect was not different between groups (significant effect "Path Length" and no interaction "Group*Path Length", Table 3, Figure 2A). Second, the effect of path width on imagery times differed for the different tasks, which was not different between groups (significant "Task*Path Width" interaction, no interaction "Task*Path Width*Group, Table 3, Figure 2B). A smaller path width resulted in longer imagery times in the MI task ($F(1,42) = 17.7$, $p<0.001$), but had no effect on imagery times in the VI task ($F(1,42) = 0.4$, $p = 0.52$). Actual and imagined walking times were significantly correlated, both in controls (Spearman's rho = 0.78, $p<0.001$) and in patients (rho = 0.54, $p<0.001$). The correlation was also significant for the freezer and non-freezers subtype separately (freezers: rho = 0.77, $p<0.001$, non-freezers: rho = 0.53, $p<0.001$).

Electromyography

There were no differences in EMG activity between VI and MI (effect "Task" $F(1,43) = 1.7$, $p = 0.20$). Patients showed more EMG activity than controls (effect "Group" $F(1,43) = 5.4$, $p = 0.03$). Crucially, there were no differences in EMG activity between the two groups (controls, patients) across tasks (analysis 1: "Task*Group" interaction: $F(1,43) = 1.3$, $p = 0.26$), nor between freezers and non-freezers across task (analysis 2: "Task*Group" interaction: $F(1,22)<1$, $p = 0.50$). Hence, differences in actual movements (related

to tremor or overt leg movements during motor imagery of gait) did not account for changes in differential (MI compared to VI) cerebral activity between groups.

Cerebral activity during motor imagery of gait for each group

Controls and patients (analysis 1)

We could confirm the presence of significant motor imagery effects in controls (cMI>cVI) in those areas previously reported in young healthy controls (Bakker *et al.,* 2008) [cMI>cVI; ROI analysis; left and right SMA, left and right superior parietal lobule (SPL), right anterior cingulate lobule, left putamen; for statistical data see supplementary material]. In the patient group, there was a significant effect of motor imagery in the right SMA [pMI>pVI; ROI-analysis, see supplementary material – Table 1]. Furthermore, a post-hoc analysis assessing the cerebral effects evoked during MI of walking (as compared to the baseline provided by the inter-trial epochs) revealed clear responses in other portions of the known locomotor network (Jahn *et al.,* 2008), in particular cerebellar and striatal regions, in both patients and controls (Supplementary material - section 8, Table 2, Figure 2).

Non-freezers and freezers (analysis 2)

In non-freezers, activity in both the right and the left SMA was larger during motor imagery than during visual imagery [nfMI>nfVI; ROI-analysis; see supplementary material]. In freezers, none of the areas previously reported were significantly activated during motor imagery [fMI>fVI; ROI-analysis], but whole-brain analysis revealed a strong effect in the posterior mid-mesencephalon (mesencephalic locomotor region (MLR), local maximum [2 -30 -18], cluster-size = 330, Z = 5.2, p (cluster-level corrected) = 0.004).

Differential cerebral activity during motor imagery of gait across groups

Controls and patients (analysis 1)

ROI analysis of the differential motor imagery-related activity of controls compared to patients [(cMI>cVI) > (pMI>pVI)], revealed a reduced activity in patients compared to controls in the SPL (Brodmann areas 5L and 7) and in the anterior cingulate cortex (caudal cingulate motor area (CMA), Brodmann area 24) (Figure 3; Table 4) (Scheperjans *et al.,* 2008; Picard and Strick, 1996).

Non-freezers and freezers (analysis 2)

Comparing non-freezers to freezers [(nfMI>nfVI) > (fMI>fVI); ROI-analysis], there was no above-threshold between-group difference, although there was a statistical trend towards increased activity in non-freezers compared to freezers in the left SMA (Brodmann area 6) and the right SPL (Figure 3 and 4; Table 4). Comparing freezers to non-freezers [(fMI>fVI) > (nfMI>nfVI); whole brain analysis], there was increased imagery-related activity in the posterior mid-mesencephalon of freezers (Figure 4; Table 4).
The maximum of the cluster was located dorsomedial to the pedunculopontine nucleus (PPN), just including the PPN (Zrinzo *et al.,* 2008). The cuneiform nucleus and the periaqueductal grey were included in the cluster (Keren *et al.,* 2009; Eippert *et al.,* 2009). The locus coeruleus is located on the lower-dorsal border of our cluster (Keren *et al.,* 2009). The mesencephalic locomotor region (MLR) is a neurophysiologically defined region which includes the PPN, cuneiform nucleus, periaqueductal grey and locus coeruleus (Jordan, 1998). The activity we found most likely includes several nuclei of the MLR, especially the cuneiform nucleus and the periaqueductal grey.

Specific effects of environmental constraints on cerebral activity during motor imagery

We found no significant differential activity for motor imagery of gait along a narrow compared to a broad path, nor was there a "Group*Task" interaction for Path width.

Brain-disease, brain-behaviour, and structural-functional relationships

Differential MLR activity in freezers (MI minus VI) correlated to FOG severity as measured by part 2 of the NFOG-Q (Figure 5A, r = 0.60, p = 0.041). MLR activity correlated to disease duration, only significantly when taking both patient groups into account (Figure 5B, freezers r = 0.53, p = 0.08, all patients r = 0.58, p = 0.003). Motor imagery-related activity (MI>VI) in the SMA was associated with greater step length (GLM effect STEP LENGTH Wald Chi Square 41.0, p<0.001, Post-hoc ANOVA showed a significant relation between SMA activity and step length in controls (F(1,14) = 9.6, r2 = 0.38, p = 0.01) but not in freezers (F(1,8)<1, r2 = 0.10, p = 0.71 after removal of outlier) or non-freezers (F(1,9) = 2.9, r2 = 0.26, p = 0.12. Motor imagery-related activity (MI>VI) in the MLR, SPL or CMA was not associated with step length or gait asymmetry.

There were no differences in global grey matter (GM), white matter (WM), or CSF volume between groups (patients versus controls; freezers versus non-freezers) (VBM Analysis 1: GM: F(1,41) = 0.753, p =

0.391; WM: F(1,41) = 0.215, p = 0.645; CSF: F(1,41) = 0.329, p = 0.569; Analysis 2: GM: F(1,20) = 0.401, p = 0.534; WM: F(1,20) = 0.321, p = 0.577; CSF: F(1,20) = 0.406, p = 0.531). The analysis of regional volume differences between groups did not show any differences in local grey matter, white matter or CSF between groups at a whole-brain corrected threshold of $p<0.05$. When focusing on the MLR cluster found in the comparison between freezers and non-freezers [(fMI>fVI)>(nfMI>nfVI)], there was a significantly larger grey matter volume in the latter group [2, -33, -18; Z = 2.89, p (voxel-level corrected) = 0.028, Figure 4, Figure 1 Supplementary Material]. The magnitude of this structural difference did not correlate to FOG severity (r = 0.28, p = 0.37). Crucially, the gait-related difference found in the MLR did not correlate to the proportion of grey matter in this same region (MI vs VI; r = 0.17, p = 0.60, Figure 5C). This indicates that differential brain atrophy between the freezers and non-freezers groups cannot account for the gait-related differences we observed in this region.

DISCUSSION

We used motor imagery to investigate alterations in cerebral activity related to planning of walking in PD patients with or without FOG. We showed that the MLR, just dorsomedial to the PPN, contributed to motor imagery of gait in freezers but not in non-freezers or controls. This altered cerebral activity was not confounded by the effects of altered motor execution, somatosensory processing, task performance or brain atrophy, and it was related to subjective FOG severity. In addition, controls and non-freezers recruited the SMA during motor imagery of gait, while freezers did not. Freezers and non-freezers, taken together, showed less motor imagery-related activity in the superior parietal lobule (Brodmann areas 5L and 7) and in the anterior cingulate cortex (Brodmann area 24) than controls.

Increased gait-related activity

Mesencephalic locomotor region

PD patients with FOG solved the motor imagery task by evoking additional activity in the posterior mid-mesencephalon. This region includes several components of the MLR, namely the PPN, the cuneiform nucleus and the periaqueductal grey. The PPN has been implied in the pathophysiology of akinesia and gait disorders in PD, based on several observations. In animal experiments and human case studies, lesions of the PPN yield akinesia, while stimulation or disinhibition of the PPN alleviates akinesia (Masdeu *et al.,* 1994;

Pahapill and Lozano, 2000; Plaha and Gill, 2005; Stefani *et al.,* 2007). Direct electrical stimulation of the PPN in humans has so-far resulted in only modest and non-significant effects on gait (Ferraye *et al.,* 2010). Analysis of electrode positions among the few patients that received the greatest benefit from PPN stimulation suggested that a more posterior stimulation may afford greater beneficial effects on gait (Pollak, 2010; Ferraye *et al.,* 2010). In another study, this more posterior part of the mesencephalon was activated by mimicked gait in PD patients (Piallat *et al.,* 2009). Those findings suggest that either the PPN lies more posterior than previously suspected, or that the subcuneiform/cuneiform nucleus was stimulated. The cluster found in the present study included the PPN, with the local maximum located in the cuneiform nucleus, and reaching the periaqueductal grey, a structure severely affected by PD (Braak *et al.,* 2000; Zweig *et al.,* 1989). We also found grey matter atrophy in the MLR in freezers compared to non-freezers, although this did not account for the differences in gait-related MLR activity. Taken together, these observations suggest that the MLR, and in particular the cuneiform nucleus and the periaqueductal grey, may be involved in FOG.

Compensation or pathology?

The MLR is recruited during actual gait in humans (Hanakawa *et al.,* 1999). Output from this structure is likely inhibited during motor imagery of gait, to prevent the MLR from driving the actual walking generators (Kaas *et al.,* 2010). Accordingly, the increased gait-related MLR activity we observed in PD patients with FOG may be pathological, reflecting a decreased inhibition from the basal ganglia. Other findings support this interpretation. First, increased MLR activity was associated with higher subjective FOG severity scores. Second, the magnitude of MLR activity evoked during motor imagery of gait was correlated to disease duration. This finding fits with the observation that longer disease duration increases the likelihood of developing FOG (Macht *et al.,* 2007), with the MLR becoming more affected as PD progresses (Braak *et al.,* 2000). Third, ischemic lesions in the dorsomedial MLR cause gait ataxia, but not a hypokinetic-rigid gait (Hathout and Bhidayasiri, 2005).

However, if gait-related activity in the MLR of freezers were exclusively pathological in nature, then how could freezers have solved the task as adequately as non-freezers and controls, despite their altered cortical responses during imagery of gait? This could point to a possible compensatory role of the MLR. This possibility is supported by recent findings, showing increased MLR activity when healthy controls perform motor imagery of gait involving frequently repeated periods of gait initiation and termination, but less

prominent activation during stable gait (la Fougere *et al.,* 2009). The latter finding fits with the absence of gait-related MLR activity in our controls, who also imagined a stable gait. Crucially, we showed that patients with FOG deviate from this pattern, showing strong MLR activity even during imagery of stable gait. This observation also fits with the increased MLR electrophysiological activity observed in freezers during mimicked stepping movements (Piallat *et al.,* 2009). Taken together, these findings suggest that the MLR might play both a compensatory and a pathological role, dependent on the computational demands imposed on this structure and on disease progression. We speculate that early in the disease, possibly even at a pre-symptomatic stage (Buhmann *et al.,* 2005), medial frontal areas (SMA) of prospective freezers fail to regulate step length. At such early stages, increased MLR activity could play a compensatory role, supporting gait planning and execution. However, the MLR ability to control gait may be limited, especially when the structure becomes more severely affected with disease progression. Additional requirements to finely adapt gait parameters to time-varying demands, as during turning and step initiation, might then lead to a collapse of this compensatory system. This scenario would reconcile a compensatory role of the MLR during stable gait, with a pathological contribution under more demanding circumstances.

Decreased gait-related cortical activity

Cingulate and supplementary motor areas

Gait-related activity in the caudal CMA was decreased in PD patients compared to controls. The caudal CMA is involved in updating and switching action plans (Rushworth *et al.,* 2002; Helmich *et al.,* 2009). We suggest that alteration of gait-related CMA activity might create a pre-condition for the manifestation of FOG, limiting the ability of PD patients to switch between motor programs. This is especially required by situations that require rapid gait adjustments like turning and step initiation.

Failures in additional gait-related cerebral structures may be necessary to actually evoke FOG. One example is the SMA. Differently from controls and non-freezers, PD patients with FOG solved the motor imagery task without evoking additional activity in the SMA, as compared to a visual imagery control task. The observed cluster falls within the portion of the SMA concerned with leg movements (Fink *et al.,* 1997). Hypoactivity in the SMA is associated with hypokinesia in PD (Nachev *et al.,* 2008; Sabatini *et al.,* 2000), and movement amplitude in PD patients improves when SMA activity is normalized (e.g. after medication, motor cortex stimulation, or deep brain stimulation) (Nachev *et al.,* 2008; Tani *et al.,* 2007; Ballanger *et al.,*

2009; Fasano *et al.,* 2008). Furthermore, decreased SMA activity is related to higher cadence and decreased step length in PD patients (Hanakawa *et al.,* 1999). Accordingly, in this study we show a relation between brain activity in the SMA (during motor imagery) and step length (during actual walking outside the scanner). These findings suggest that the decreased SMA activity observed in freezers may be related to altered regulation of step amplitude. The emphasis here is on abnormal regulation, since freezers could produce step amplitudes largely overlapping with those of non-freezers and controls. As such, this finding qualifies the hypothesis that a failure to generate steps of adequate amplitude could lead to a progressive decrease in step amplitude, and ultimately produce FOG (Chee *et al.,* 2009).

Superior parietal lobule

During motor imagery of gait, cerebral activity in the right SPL was reduced in patients compared to controls. This confirms previous SPECT findings related to gait execution in PD (Hanakawa *et al.,* 1999). We suggest that the reduced activity in the SPL of PD patients during imagery of gait underlies their difficulty in predicting the somatosensory consequences of a motor plan (Blakemore and Sirigu, 2003; Wolpert *et al.,* 1998). This interpretation fits with the known impairments of PD patients in integrating proprioceptive information into a motor plan (Lewis and Byblow, 2002; Almeida *et al.,* 2005; Keijsers *et al.,* 2005).

Interpretational issues

Patients were classified as 'freezers' when there was an evident history of FOG. All freezers reported the characteristic gluing of the feet, and recognised the typical phenotype when this was demonstrated to them. Most patients also showed FOG during neurological examination. We included patients with relatively mild FOG, as this facilitated a proper match between freezers and non-freezers with respect to disease severity and duration. This may explain why three patients with mild freezing did not demonstrate FOG during clinical examination, despite convincing subjective accounts of FOG. Post-hoc exploratory analyses suggested that the MLR activation in these patients without objective FOG was intermediate between fully overt freezers and non-freezers, perhaps reflecting a spectrum of severity (data not shown).

All three groups performed the task proficiently, without overall differences in imagery times between groups. Non-freezers showed a trend towards slower imagery times, but this included both the motor imagery and visual imagery task. Hence, this tendency for different imagery times cannot explain the differential

(MI>VI) functional brain activity. Moreover, in all groups imagery times were equally sensitive to the length and width of the path and correlated to actual walking times. These findings indicate that both patients and controls were equally effective in solving the motor imagery task. This excludes task difficulty as an explanation for between-group cerebral differences during motor imagery.

The basal ganglia are affected in PD, and are involved in motor imagery of gait in young healthy subjects (Bakker *et al.,* 2008). Moreover, other studies have suggested that failure of the caudate nucleus may contribute to FOG (Bartels *et al.,* 2006). However, we found no differences in cerebral activity in the basal ganglia between patients and controls. This is likely a sign of the extreme selectivity of our functional comparison (MI vs. VI), rather than a lack of sensitivity (see Supplementary Table 2, Figure 2).

Conclusions

We have shown that PD patients with FOG performing motor imagery of gait use different cerebral structures than matched PD patients without FOG or healthy controls. These cerebral differences were observed in the context of matched behavioural performance across groups, and could not be explained by brain atrophy. During imagined walking, PD patients with FOG showed increased activity in the MLR, which was related to subjective FOG severity. In addition, PD patients with FOG tended to have reduced activity in mesial frontal and posterior parietal regions. These findings provide new insights into the pathophysiology of FOG: the cause of FOG may be altered cortical regulation of movement execution, together with a progressively impaired ability of mesencephalic structures to flexibly compensate for that alteration. This may explain the manifestation of FOG during changes in motor behaviour, such as turning or initiating walking. These gait adaptations not only require a switch of motor program, but also more precise regulation of step length and gait timing.

Snijders; motor imagery and freezing of gait

Legend to the figures

Figure 1. Task setup. A) Examples of photographs of walking trajectories presented to the subjects during motor imagery (MI), and visual imagery (VI) experiments. The photographs show a corridor with a white path in the middle and a green pillar positioned on the path. During MI trials, a green square is present at the beginning of the path. During VI trials, a black disc is present at the beginning of the path. During both tasks, the path width can be either broad, or narrow. In addition, the green pillar can be positioned at 2, 4, 6, 8 or 10 m from the start marker (2 m is presented in the photos of this figure). **B)** Time course of motor imagery trials. During each trial, after a short inspection of the photo on display, the subjects closed their eyes and imagined standing on the left side of the path, next to the green square. The subjects were asked to press a button with the index finger of their left or right hand to signal that they had started imagining stepping onto the path and walking along the path. The subjects were also asked to press the button again when they imagined having reached the end of the walking trajectory. Following the second button press, a fixation cross was presented on the screen and the subjects could open their eyes. The duration of the inter-trial interval (ITI) was 4-12 s.

Figure 2. Behavioural performance during scanning. Average imagery times (±SEM) measured in freezers, non-freezers and controls. MI = motor imagery, VI = visual imagery. **A)** Imagery times for trials with different path lengths [2, 4, 6, 8, and 10 m] and **B)** for trials with different path widths [broad, narrow].

Figure 3. Imagery-related brain activity. Brain areas in which the relative increase in activity for motor imagery (MI) versus visual imagery (VI) was greater in controls than patients (ROI-analysis, $p<0.05$ corrected for multiple comparisons using family-wise inference on voxel level). **A)** Statistical parametric maps (SPM) of increased activity in the right superior parietal lobule (SPL) and right anterior cingulate cortex (cingulated motor area; CMA), superimposed on a sagittal brain section (top panel SPL, bottom panel CMA). **B)** Beta weights of the contrast between motor imagery and visual imagery (mean ± SEM) from right SPL cluster (top panel) and the right CMA cluster (bottom panel) in controls, non-freezers and freezers.

Figure 4. Imagery-related brain activity. Brain areas in which the relative increase in activity for motor imagery (MI) versus visual imagery (VI) differed between freezers and non-freezers (Supplementary motor

cortex (SMA): ROI analysis, p = 0.06 corrected for multiple comparisons using family-wise inference on voxel level; Mesencephalic locomotor region (MLR) whole brain search, p<0.05 corrected for multiple comparisons using family-wise error (cluster-level). **A)** SPM of decreased activity in the SMA and increased activity in the MLR**,** superimposed on a sagittal brain section (top left panel SMA, middle left panel MLR) and a transversal brain section (top right panel SMA, middle left panel MLR). The bottom brain sections include the small cluster with significant difference in grey matter between freezers and non-freezers in the MLR **B)** Beta weights of the contrast between motor imagery and visual imagery (mean ± SEM) from the SMA cluster (top panel) and the MLR cluster (bottom panel) in controls, non-freezers and freezers.

Figure 5. Brain-disease and structural-functional relationships. Relation between differential cerebral activity and clinical/structural parameters in freezers. **A)** Scatterplot of beta weights of the contrast between motor imagery and visual imagery from the mesencephalic locomotor region (MLR) cluster (y-axis) against score on the New Freezing of Gait Questionnaire part 2 (N-FOGQ; x-axis; Pearson's correlation r = 0.60, p = 0.04) **B)** Scatterplot of beta weights of the contrast between motor imagery and visual imagery from the MLR cluster (y-axis) against disease duration (in years; x-axis; r = 0.53, p = 0.08) **C)** Scatterplot of beta weights of the contrast between motor imagery and visual imagery from the MLR cluster (y-axis) against grey matter volume (in ml) of the same cluster (x-axis; r = -0.17, p = 0.44).

Acknowledgements:

This research was supported by the Netherlands Organization for Scientific Research (NWO) [016076352 to B.B., 45203339 to I.T., 92003490 to A.S., 91656103 to S.O.] and by the Stichting Internationaal Parkinson Fonds. R.H. was supported by a grant from the Alkemade-Keuls foundation.

We would like to thank Paul Gaalman for his expert assistance during scanning, Lennart Verhagen for his SPM assistance and Charlotte Haaxma for rating the video's on FOG. In addition, we would like to thank Alan Pieterse for assistance using the GaitRite.

Reference List

Almeida QJ, Frank JS, Roy EA, Jenkins ME, Spaulding S, Patla AE*, et al*. An evaluation of sensorimotor integration during locomotion toward a target in Parkinson's disease. Neuroscience 2005; 134: 283-293.

Ashburner J, Friston KJ. Voxel-based morphometry--the methods. Neuroimage 2000; 11: 805-821.

Bakker M, de Lange FP, Helmich RC, Scheeringa R, Bloem BR, Toni I. Cerebral correlates of motor imagery of normal and precision gait. Neuroimage 2008; 41: 998-1010.

Bakker M, de Lange FP, Stevens JA, Toni I, Bloem BR. Motor imagery of gait: a quantitative approach. Exp Brain Res 2007a; 179: 497-504.

Bakker M, Verstappen CC, Bloem BR, Toni I. Recent advances in functional neuroimaging of gait. J Neural Transm 2007b; 114: 1323-1331.

Ballanger B, Lozano AM, Moro E, van ET, Hamani C, Chen R*, et al*. Cerebral blood flow changes induced by pedunculopontine nucleus stimulation in patients with advanced Parkinson's disease: A [(15)O] H(2)O PET study. Hum Brain Mapp 2009; 30: 3901-3909.

Bartels AL, de Jong BM, Giladi N, Schaafsma JD, Maguire RP, Veenma L*, et al*. Striatal dopa and glucose metabolism in PD patients with freezing of gait. Mov Disord 2006; 21: 1326-1332.

Blakemore SJ, Sirigu A. Action prediction in the cerebellum and in the parietal lobe. Exp Brain Res 2003; 153: 239-245.

Bloem BR, Hausdorff JM, Visser JE, Giladi N. Falls and freezing in Parkinson's disease: a review of two interconnected, episodic phenomena. Mov Disord 2004; 19: 871-884.

Braak H, Rub U, Sandmann-Keil D, Gai WP, de Vos RA, Jansen Steur EN*, et al*. Parkinson's disease: affection of brain stem nuclei controlling premotor and motor neurons of the somatomotor system. Acta Neuropathol 2000; 99: 489-495.

Buhmann C, Binkofski F, Klein C, Buchel C, van ET, Erdmann C*, et al*. Motor reorganization in asymptomatic carriers of a single mutant Parkin allele: a human model for presymptomatic parkinsonism. Brain 2005; 128: 2281-2290.

Chee R, Murphy A, Danoudis M, Georgiou-Karistianis N, Iansek R. Gait freezing in Parkinson's disease and the stride length sequence effect interaction. Brain 2009; 132: 2151-2160.

Cisek P, Kalaska JF. Neural correlates of mental rehearsal in dorsal premotor cortex. Nature 2004; 431: 993-996.

de Lange FP, Helmich RC, Toni I. Posture influences motor imagery: an fMRI study. Neuroimage 2006; 33: 609-617.

Duvernoy HM, Cabanis EA, Vannson JL. The human brain: surface, and three-dimensional sectional anatomy and MRI. Vienna: Springer; 1991.

Eickhoff SB, Stephan KE, Mohlberg H, Grefkes C, Fink GR, Amunts K*, et al*. A new SPM toolbox for combining probabilistic cytoarchitectonic maps and functional imaging data. Neuroimage 2005; 25: 1325-1335.

Eippert F, Bingel U, Schoell ED, Yacubian J, Klinger R, Lorenz J*, et al*. Activation of the opioidergic descending pain control system underlies placebo analgesia. Neuron 2009; 63: 533-543.

Fabre N, Brefel C, Sabatini U, Celsis P, Montastruc JL, Chollet F*, et al*. Normal frontal perfusion in patients with frozen gait. Mov Disord 1998; 13: 677-683.

Fasano A, Piano C, De SC, Cioni B, Di GD, Zinno M*, et al*. High frequency extradural motor cortex stimulation transiently improves axial symptoms in a patient with Parkinson's disease. Mov Disord 2008; 23: 1916-1919.

Ferraye MU, Debu B, Fraix V, Goetz L, Ardouin C, Yelnik J, *et al*. Effects of pedunculopontine nucleus area stimulation on gait disorders in Parkinson's disease. Brain 2010; 133: 205-214.

Field A. Discovering statistics using SPSS. London: SAGE publications Ltd; 2009.

Fink GR, Frackowiak RS, Pietrzyk U, Passingham RE. Multiple nonprimary motor areas in the human cortex. J Neurophysiol 1997; 77: 2164-2174.

Friston KJ, Holmes A, Poline JB, Price CJ, Frith CD. Detecting activations in PET and fMRI: levels of inference and power. Neuroimage 1996; 4: 223-235.

Friston KJ, Holmes AP, Poline JB, Grasby PJ, Williams SC, Frackowiak RS, *et al*. Analysis of fMRI time-series revisited. Neuroimage 1995; 2: 45-53.

Gentili R, Cahouet V, Ballay Y, Papaxanthis C. Inertial properties of the arm are accurately predicted during motor imagery. Behav Brain Res 2004; 155: 231-239.

Hanakawa T, Katsumi Y, Fukuyama H, Honda M, Hayashi T, Kimura J, *et al*. Mechanisms underlying gait disturbance in Parkinson's disease: a single photon emission computed tomography study. Brain 1999; 122 (Pt 7): 1271-1282.

Hathout GM, Bhidayasiri R. Midbrain ataxia: an introduction to the mesencephalic locomotor region and the pedunculopontine nucleus. AJR Am J Roentgenol 2005; 184: 953-956.

Hausdorff JM, Schaafsma JD, Balash Y, Bartels AL, Gurevich T, Giladi N. Impaired regulation of stride variability in Parkinson's disease subjects with freezing of gait. Exp Brain Res 2003; 149: 187-194.

Helmich RC, Aarts E, de Lange FP, Bloem BR, Toni I. Increased dependence of action selection on recent motor history in Parkinson's disease. J Neurosci 2009; 29: 6105-6113.

Hughes AJ, Daniel SE, Kilford L, Lees AJ. Accuracy of clinical diagnosis of idiopathic Parkinson's disease: a clinico-pathological study of 100 cases. J Neurol Neurosurg Psychiatry 1992; 55: 181-184.

Isaac I, Marks DF, Russell DG. An instrument for assessing imagery of movement: the vividness of movement imagery questionnaire (VMIQ). J Ment Imag 1986; 23-30.

Jacobs JV, Lou JS, Kraakevik JA, Horak FB. The supplementary motor area contributes to the timing of the anticipatory postural adjustment during step initiation in participants with and without Parkinson's disease. Neuroscience 2009a; 164: 877-885.

Jacobs JV, Nutt JG, Carlson-Kuhta P, Stephens M, Horak FB. Knee trembling during freezing of gait represents multiple anticipatory postural adjustments. Exp Neurol 2009b; 215: 334-341.

Jahn K, Deutschlander A, Stephan T, Kalla R, Wiesmann M, Strupp M, *et al*. Imaging human supraspinal locomotor centers in brainstem and cerebellum. Neuroimage 2008; 39: 786-792.

Jeannerod M. The representing brain: Neural correlates of motor intention and imagery. Behavioral Brain Sciences 1994; 17: 187-245.

Jordan LM. Initiation of locomotion in mammals. Ann N Y Acad Sci 1998; 860: 83-93.

Kaas A, Weigelt S, Roebroeck A, Kohler A, Muckli L. Imagery of a moving object: the role of occipital cortex and human MT/V5+. Neuroimage 2010; 49: 794-804.

Keijsers NL, Admiraal MA, Cools AR, Bloem BR, Gielen CC. Differential progression of proprioceptive and visual information processing deficits in Parkinson's disease. Eur J Neurosci 2005; 21: 239-248.

Keren NI, Lozar CT, Harris KC, Morgan PS, Eckert MA. In vivo mapping of the human locus coeruleus. Neuroimage 2009; 47: 1261-1267.

la Fougere C, Zwergal A, Rominger A, Forster S, Fesl G, Dieterich M, *et al*. Real versus imagined locomotion: A [(18)F]-FDG PET-fMRI comparison. Neuroimage 2009.

Lewis GN, Byblow WD. Altered sensorimotor integration in Parkinson's disease. Brain 2002; 125: 2089-2099.

Macht M, Kaussner Y, Moller JC, Stiasny-Kolster K, Eggert KM, Kruger HP, *et al*. Predictors of freezing in Parkinson's disease: a survey of 6,620 patients. Mov Disord 2007; 22: 953-956.

Malouin F, Richards CL, Jackson PL, Dumas F, Doyon J. Brain activations during motor imagery of locomotor-related tasks: a PET study. Hum Brain Mapp 2003; 19: 47-62.

Masdeu JC, Alampur U, Cavaliere R, Tavoulareas G. Astasia and gait failure with damage of the pontomesencephalic locomotor region. Ann Neurol 1994; 35: 619-621.

Matsui H, Udaka F, Miyoshi T, Hara N, Tamaura A, Oda M, *et al*. Three-dimensional stereotactic surface projection study of freezing of gait and brain perfusion image in Parkinson's disease. Mov Disord 2005; 20: 1272-1277.

Mayka MA, Corcos DM, Leurgans SE, Vaillancourt DE. Three-dimensional locations and boundaries of motor and premotor cortices as defined by functional brain imaging: a meta-analysis. Neuroimage 2006; 31: 1453-1474.

Miller KJ, Schalk G, Fetz EE, den NM, Ojemann JG, Rao RP. Cortical activity during motor execution, motor imagery, and imagery-based online feedback. Proc Natl Acad Sci U S A 2010; 107: 4430-4435.

Mulder T, Hochstenbach JB, van Heuvelen MJ, den Otter AR. Motor imagery: the relation between age and imagery capacity. Hum Mov Sci 2007; 26: 203-211.

Nachev P, Kennard C, Husain M. Functional role of the supplementary and pre-supplementary motor areas. Nat Rev Neurosci 2008; 9: 856-869.

Nico D, Daprati E, Rigal F, Parsons L, Sirigu A. Left and right hand recognition in upper limb amputees. Brain 2004; 127: 120-132.

Nieuwboer A, Dom R, De WW, Desloovere K, Janssens L, Stijn V. Electromyographic profiles of gait prior to onset of freezing episodes in patients with Parkinson's disease. Brain 2004; 127: 1650-1660.

Nieuwboer A, Rochester L, Herman T, Vandenberghe W, Emil GE, Thomaes T, *et al*. Reliability of the new freezing of gait questionnaire: agreement between patients with Parkinson's disease and their carers. Gait Posture 2009; 30: 459-463.

Pahapill PA, Lozano AM. The pedunculopontine nucleus and Parkinson's disease. Brain 2000; 123 (Pt 9): 1767-1783.

Piallat B, Chabardes S, Torres N, Fraix V, Goetz L, Seigneuret E, *et al*. Gait is associated with an increase in tonic firing of the sub-cuneiform nucleus neurons. Neuroscience 2009; 158: 1201-1205.

Picard N, Strick PL. Motor areas of the medial wall: a review of their location and functional activation. Cereb Cortex 1996; 6: 342-353.

Plaha P, Gill SS. Bilateral deep brain stimulation of the pedunculopontine nucleus for Parkinson's disease. Neuroreport 2005; 16: 1883-1887.

Plotnik M, Giladi N, Hausdorff JM. Bilateral coordination of walking and freezing of gait in Parkinson's disease. Eur J Neurosci 2008; 27: 1999-2006.

Pollak P. 2010.

Price CJ, Friston KJ. Functional imaging studies of neuropsychological patients: applications and limitations. Neurocase 2002; 8: 345-354.

Rushworth MF, Hadland KA, Paus T, Sipila PK. Role of the human medial frontal cortex in task switching: a combined fMRI and TMS study. J Neurophysiol 2002; 87: 2577-2592.

Sabatini U, Boulanouar K, Fabre N, Martin F, Carel C, Colonnese C*, et al*. Cortical motor reorganization in akinetic patients with Parkinson's disease: a functional MRI study. Brain 2000; 123 (Pt 2): 394-403.

Scheperjans F, Eickhoff SB, Homke L, Mohlberg H, Hermann K, Amunts K*, et al*. Probabilistic maps, morphometry, and variability of cytoarchitectonic areas in the human superior parietal cortex. Cereb Cortex 2008; 18: 2141-2157.

Snijders AH, Nijkrake MJ, Bakker M, Munneke M, Wind C, Bloem BR. Clinimetrics of freezing of gait. Mov Disord 2008; 23 Suppl 2: S468-S474.

Stefani A, Lozano AM, Peppe A, Stanzione P, Galati S, Tropepi D*, et al*. Bilateral deep brain stimulation of the pedunculopontine and subthalamic nuclei in severe Parkinson's disease. Brain 2007; 130: 1596-1607.

Stephan KM, Fink GR, Passingham RE, Silbersweig D, Ceballos-Baumann AO, Frith CD*, et al*. Functional anatomy of the mental representation of upper extremity movements in healthy subjects. J Neurophysiol 1995; 73: 373-386.

Tani N, Saitoh Y, Kishima H, Oshino S, Hatazawa J, Hashikawa K*, et al*. Motor cortex stimulation for levodopa-resistant akinesia: case report. Mov Disord 2007; 22: 1645-1649.

Wolpert DM, Goodbody SJ, Husain M. Maintaining internal representations: the role of the human superior parietal lobe. Nat Neurosci 1998; 1: 529-533.

Zrinzo L, Zrinzo LV, Tisch S, Limousin PD, Yousry TA, Afshar F*, et al*. Stereotactic localization of the human pedunculopontine nucleus: atlas-based coordinates and validation of a magnetic resonance imaging protocol for direct localization. Brain 2008; 131: 1588-1598.

Zweig RM, Jankel WR, Hedreen JC, Mayeux R, Price DL. The pedunculopontine nucleus in Parkinson's disease. Ann Neurol 1989; 26: 41-46.

Table 1: Clinical characteristics

Parameter	Group	N	Mean	SD	P-value
Gender	Patients	24	9F/15M		0.18
	Controls	21	9F / 12M		
	Freezers	12	4F / 8M		0.22
	Non-Freezers	12	5F / 7M		
Age (years)	Patients	24	60.2	8.9	0.25
	Controls	21	57.0	9.1	
	Freezers	12	58.7	9.0	0.20
	Non-Freezers	12	62.6	7.1	
Disease duration	Freezers	12	9.8	4.6	0.10
	Non-Freezers	12	7.1	3.0	
UPDRS III	Freezers	12	34.6	9.6	0.20
	Non-Freezers	12	28.6	12.2	
FAB	Freezers	12	16.5	1.4	0.22
	Non-Freezers	12	17.1	0.8	

H&Y = Hoehn and Yahr Rating Scale; UPDRS III = Unified Parkinson's Disease Rating Scale part 3; FAB = Frontal Assessment Battery; M = Male; F = Female. Statistical inferences are based on independent samples t-test (Chi-squared test for Gender).

Table 2: Gait data

Parameter	Group	Mean	SD	P-value
Normalized step-length	Patients	0.71	0.08	0.009
	Controls	0.78	0.08	
	Freezers	0.66	0.15	0.17
	Non-Freezers	0.73	0.07	
Gait asymmetry	Patients	0.036	0.027	0.003
	Controls	0.015	0.011	
	Freezers	0.040	0.027	0.5
	Non-Freezers	0.033	0.029	

Normalized step length: Step length / leg length

Gait asymmetry: Natural logarithm (ln) of the difference in swingtime between the feet

Statistical test: independent samples t-tests.

Table 3: Behavioural performance (between-groups comparisons on imagery times)

Effect:	Patients versus Controls		Freezers versus Non-freezers	
	F (df)	p-value	F (df)	p-value
Group	< 1 (1,43)	0.35	3.7 (1,22)	0.07
Task (MI vs VI)	1.3 (1,43)	0.26	2.5 (1,22)	0.13
Task*Group	2.3 (1,43)	0.13	< 1 (1,22)	0.44
Path length	69.8 (4,172)	< 0.001	62.1 (4,88)	< 0.001
Path length * Group	1.5 (4,172)	0.23	2.8 (4,88)	0.61
Task*Path width	17.5 (1,43)	< 0.001	8.8 (1,22)	0.007
Task*Path width*Group	< 1 (1,43)	0.734	< 1 (1,22)	0.80

MI = motor imagery; VI = visual imagery

Table 4: Stereotactic coordinates of local maxima with differential cerebral activity during motor imagery of gait across groups

Contrast	*Search volume*	*Anatomical label*	*Functional label*	*Cluster size*	*Hemi-sphere*	*Z-value*	*p-value*	*x*	*y*	*z*
Analysis 1: Controls versus Patients										
(cMI>cVI) > (pMI>pVI)	ROI	Superior parietal lobule	Area 5L	144	R	3.1	0.019	14	-58	66
		Ant. cingulate cortex	Area 24	65	R	3.0	0.025	2	2	40
Analysis 2: Non-freezers versus Freezers										
(nfMI>nfVI) > (fMI>fVI)	ROI	Superior parietal lobule	Area 5L	93	R	2.6	0.074	22	-50	72
		Superior frontal gyrus	SMA	64	L	2.6	0.061	-10	-16	72
(fMI>fVI) > (nfMI>nfVI)	Whole-brain	Posterior mid-mesencephalon	Mesencephalic locomotor region	170		4.5	0.049	0	-28	-20

Results of whole-brain analysis are corrected for multiple comparisons for search over the whole brain using cluster-level family-wise inference ($p<0.05$).

Results of ROI analysis are corrected for multiple comparisons over the ROI volume using voxel-level family-wise inference ($p<0.05$).

Stereotactic coordinates are reported in Montreal Neurological Institute (MNI) space. Details on the anatomical and functional labelling can be found in the Methods and Results sections.

c = controls; f = freezers; nf = non-freezers; MI = motor imagery; VI = visual imagery; R = right; L = left; SMA = supplementary motor area

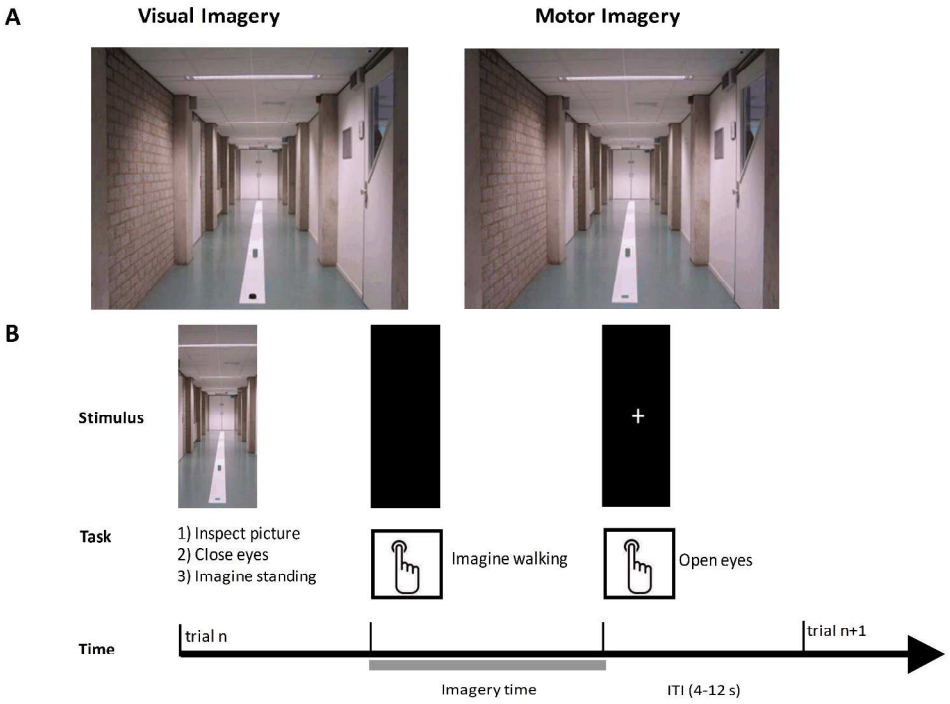

Figure 1. Task setup. A) Examples of photographs of walking trajectories presented to the subjects during motor imagery (MI), and visual imagery (VI) experiments. The photographs show a corridor with a white path in the middle and a green pillar positioned on the path. During MI trials, a green square is present at the beginning of the path. During VI trials, a black disc is present at the beginning of the path. During both tasks, the path width can be either broad, or narrow. In addition, the green pillar can be positioned at 2, 4, 6, 8 or 10 m from the start marker (2 m is presented in the photos of this figure). B) Time course of motor imagery trials. During each trial, after a short inspection of the photo on display, the subjects closed their eyes and imagined standing on the left side of the path, next to the green square. The subjects were asked to press a button with the index finger of their left or right hand to signal that they had started imagining stepping onto the path and walking along the path. The subjects were also asked to press the button again when they imagined having reached the end of the walking trajectory. Following the second button press, a fixation cross was presented on the screen and the subjects could open their eyes. The duration of the inter-trial interval (ITI) was 4-12 s.
265x188mm (600 x 600 DPI)

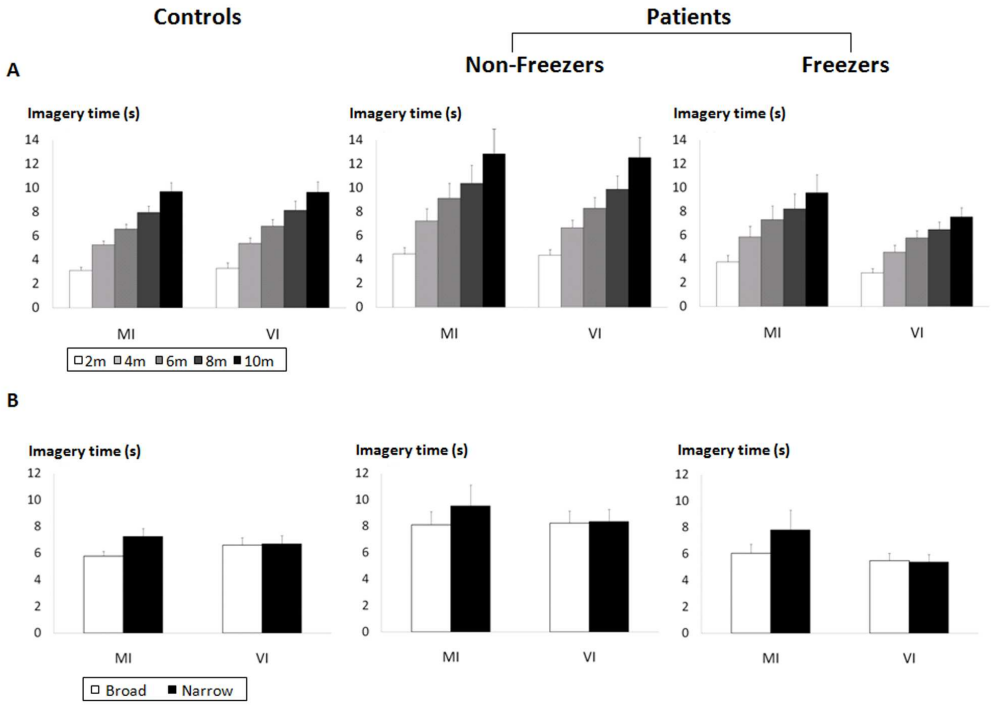

Figure 2. Behavioural performance during scanning. Average imagery times (±SEM) measured in freezers, non-freezers and controls. MI = motor imagery, VI = visual imagery. A) Imagery times for trials with different path lengths [2, 4, 6, 8, and 10 m] and B) for trials with different path widths [broad, narrow].
252x180mm (600 x 600 DPI)

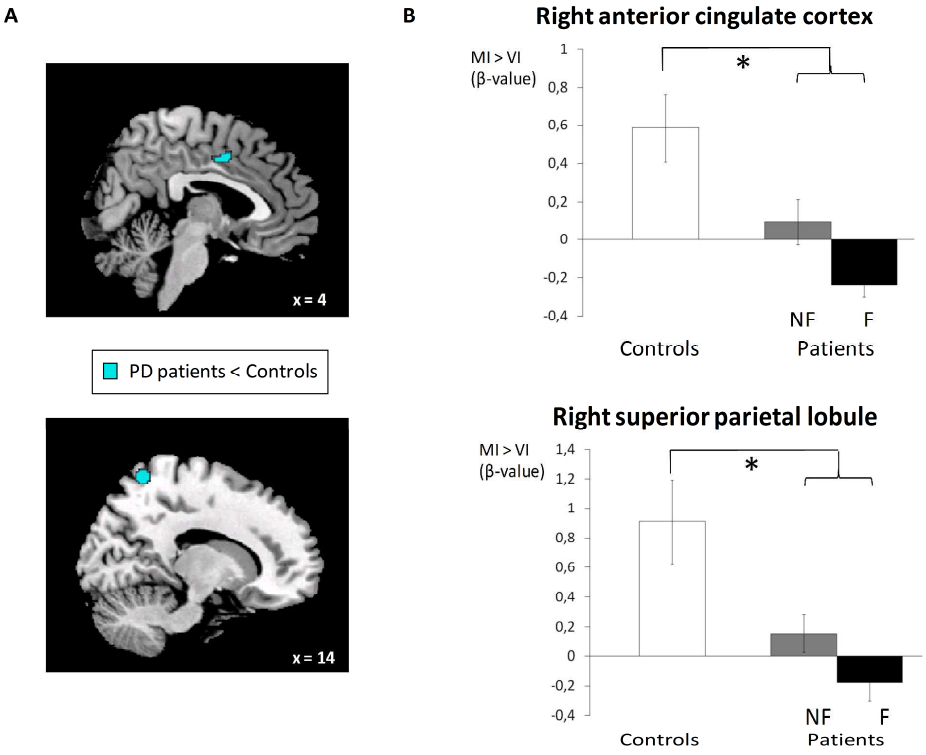

Figure 3. Imagery-related brain activity. Brain areas in which the relative increase in activity for motor imagery (MI) versus visual imagery (VI) was greater in controls than patients (ROI-analysis, $p < 0.05$ corrected for multiple comparisons using family-wise inference on voxel level). A) Statistical parametric maps (SPM) of increased activity in the right superior parietal lobule (SPL) and right anterior cingulate cortex (cingulated motor area; CMA), superimposed on a sagittal brain section (top panel SPL, bottom panel CMA). B) Beta weights of the contrast between motor imagery and visual imagery (mean ± SEM) from right SPL cluster (top panel) and the right CMA cluster (bottom panel) in controls, non-freezers and freezers.
261x199mm (600 x 600 DPI)

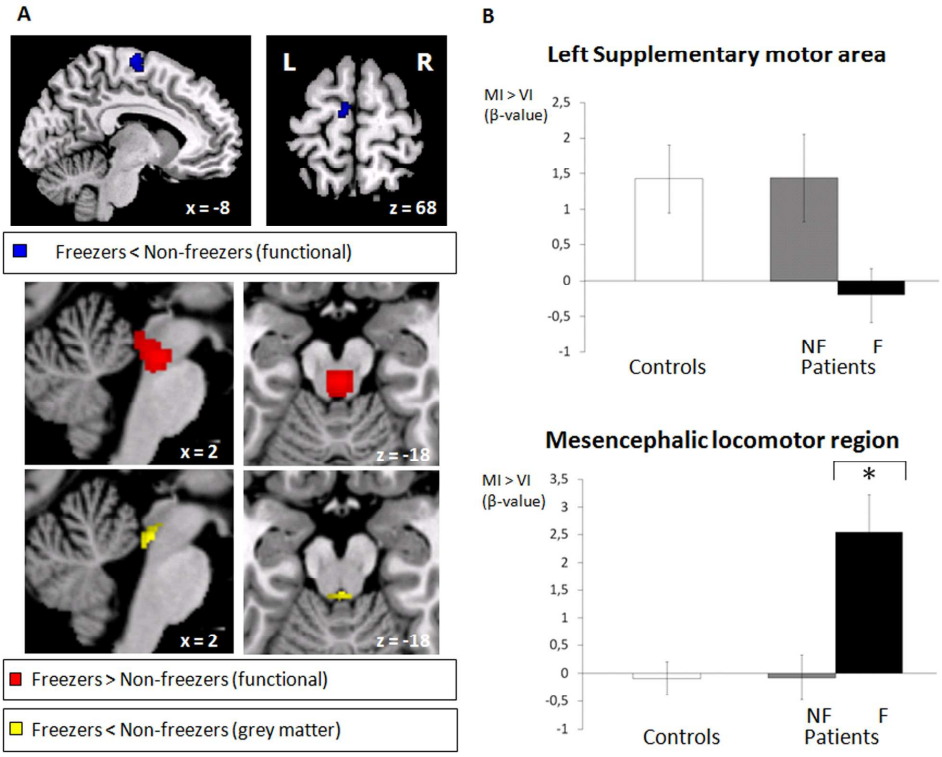

Figure 4. Imagery-related brain activity. Brain areas in which the relative increase in activity for motor imagery (MI) versus visual imagery (VI) differed between freezers and non-freezers (Supplementary motor cortex (SMA): ROI analysis, p = 0.06 corrected for multiple comparisons using family-wise inference on voxel level; Mesencephalic locomotor region (MLR) whole brain search, p<0.05 corrected for multiple comparisons using family-wise error (cluster-level). A) SPM of decreased activity in the SMA and increased activity in the MLR, superimposed on a sagittal brain section (top left panel SMA, middle left panel MLR) and a transversal brain section (top right panel SMA, middle left panel MLR). The bottom brain sections include the small cluster with significant difference in grey matter between freezers and non-freezers in the MLR B) Beta weights of the contrast between motor imagery and visual imagery (mean ± SEM) from the SMA cluster (top panel) and the MLR cluster (bottom panel) in controls, non-freezers and freezers.
177x135mm (600 x 600 DPI)

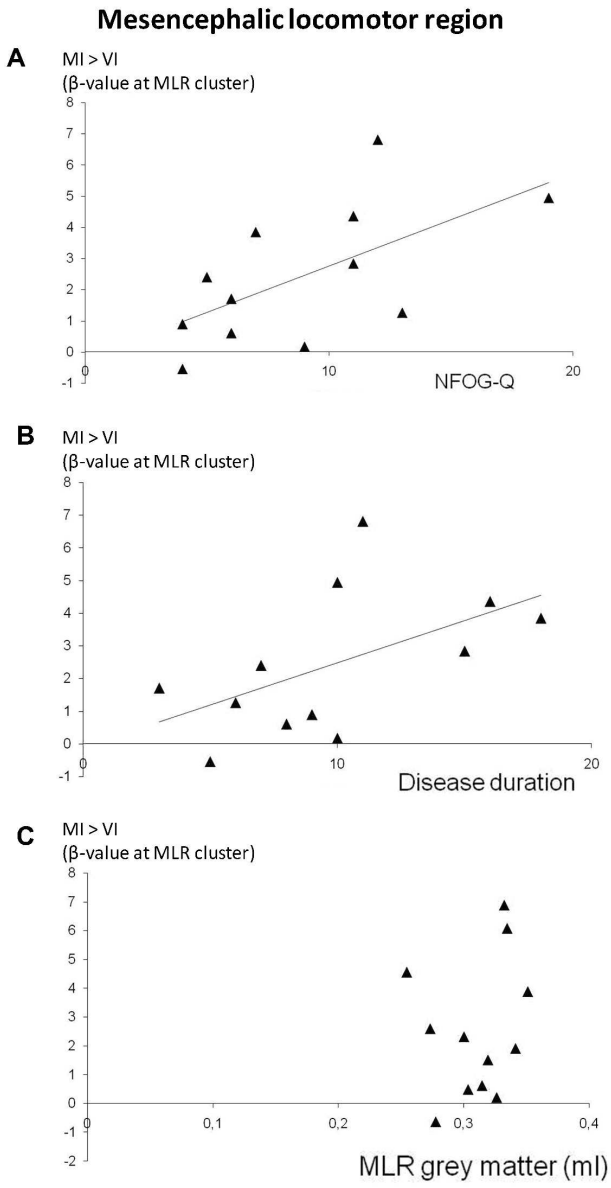

Figure 5. Brain-disease and structural-functional relationships. Relation between differential cerebral activity and clinical/structural parameters in freezers. A) Scatterplot of beta weights of the contrast between motor imagery and visual imagery from the mesencephalic locomotor region (MLR) cluster (y-axis) against score on the New Freezing of Gait Questionnaire part 2 (N-FOGQ; x-axis; Pearson's correlation r = 0.60, p = 0.04) B) Scatterplot of beta weights of the contrast between motor imagery and visual imagery from the MLR cluster (y-axis) against disease duration (in years; x-axis; r = 0.53, p = 0.08) C) Scatterplot of beta weights of the contrast between motor imagery and visual imagery from the MLR cluster (y-axis) against grey matter volume (in ml) of the same cluster (x-axis; r = -0.17, p = 0.44).
153x281mm (600 x 600 DPI)

Supplementary material

Here we describe in detail:

1. Tasks

Subjects performed two tasks: motor imagery of gait, and a matched visual imagery control task. Both tasks started with the presentation of a photograph showing a corridor with a path in the middle (Fig. 1). During the motor imagery task (MI), subjects were asked to imagine walking

along this path. During the visual imagery task (VI), subjects were asked to imagine seeing a disc moving along the path. A MI trial started with the presentation of a photograph with a green square as a start marker (Fig. 1a). Subjects were asked to briefly inspect the picture, close their eyes, imagine walking along the path (starting from the green square and stopping at the green pillar) and open their eyes when they imagined having reached the green pillar (see Fig. 1b for trial time course). Subjects were instructed to vividly imagine the walking movement, in a first person perspective, as if their legs were moving, but without making any actual movements. A VI trial started with the presentation of a photograph with a black disc as start marker (Fig. 1a). Subjects were asked to briefly inspect the picture, close their eyes, imagine standing on the left side of the beginning of the path and seeing the disc moving towards the green pillar, and to open their eyes when they imagined the disc reaching the green pillar. During both tasks, the path could have two different widths (narrow, broad). In addition, the green pillar could be placed at five different distances from the green square or the black disc (2, 4, 6, 8, and 10 m). During each trial, subjects signalled that they had started and stopped the imagery by pressing a button. Patients pressed the button with their least affected hand (17 left, 8 right). Controls were matched to the patients: i.e. 14 controls pressed the button with their left hand and 7 with their right hand. Also the freezer and non-freezer groups were matched (freezers: 9 left, 4 right ; non-freezers: 8 left, 4 right). We explicitly instructed subjects not to count during the imagery tasks.

2. Experimental procedure

During the experiment, subjects were lying supine in the MR scanner. Visual stimuli were presented by means of a PC running Presentation software (Neurobehavioural systems, Albany, USA), and were projected onto a screen at the back of the scanner. Subjects could see the screen via a mirror above their heads.

The MI and VI tasks were performed in two successive sessions of 25 minutes each, separated by a break outside the scanner. Task order was counter-balanced across subjects. For

each session, the trial order was pseudo-randomized across the experimental factors (i.e. path width (2 levels) and path length (5 levels)). We used two fixed pseudo-randomized orders that were counterbalanced across the two tasks. In between trials a fixation cross was presented (inter-trial interval, ITI: 4-12 sec).

Before each session, subjects were given written and verbal instruction about the task they were going to perform, followed by training in the relevant task outside the scanner (15 trials) and inside the MR-scanner (first session only, 7 trials). Prior to the MI task, subjects were asked to walk along short versions (three meters) of the same broad and narrow paths used in the MI task (3 times for each path width), at a comfortable pace, avoiding to place their feet outside the path. We instructed subjects to pay attention to the feeling of walking along the different path widths, and to imagine walking in a similar way along the two different paths during the imagery trials. To familiarize subjects with the movement of the disc, prior to the VI task, they saw a video of the disc moving through the same corridor as in the photographs. The disc moved for 6 m, in a straight line, at a uniform speed of about 0.8 m/s. We instructed subjects to imagine seeing the disc moving in a similar way along the two different paths during the imagery trials.

3. Data collection

Button presses were recorded with an MR-compatible keypad (MRI Devices, Waukesha, WI) positioned on the subjects' abdomen.

MR images were acquired on a Siemens 3T Trio system (Siemens, Erlangen, Germany), using an 8 channel head coil for signal reception and a body coil for radio-frequency transmission. Blood oxygenation level-dependent (BOLD) sensitive functional images were acquired using a single shot gradient EPI sequence (TR/TE = 2380 ms/30 ms; 50 ms gap between successive volumes; 35 transversal slices; ascending acquisition; voxel size 3.5 x 3.5 x 3 mm; FOV = 224 mm). High-resolution anatomical images were acquired using an MP-RAGE

sequence (TR/TE = 2300/2.92 ms, 192 sagittal slices, voxel size 1.0 x 1.0 x 1.0 mm, FOV = 256 mm).

Eye movements were measured with a video-based infrared eyetracker (Sensomotoric Instruments, Berlin, Germany). These measures allowed us to have online visual inspection of task performance.

4. EMG recordings, preprocessing and subsequent analyses

A concern that arises when comparing cerebral activity during motor imagery of gait in patients versus controls is that differences in actual movements (related to tremor or overt leg movements during motor imagery of gait) might result in changes in cerebral activity between patients and controls. To control for these factors, muscle activity from the forearm and lower leg was measured during the fMRI experiment.

Muscle activity was recorded with an MR compatible EMG (electromyography) system (Brain Products GmBH, Gilching, Germany). Silver/silver-chloride electrodes were placed three cm apart on the tibialis anterior and extensor carpi radialis in a belly tendon montage. Ground electrodes were placed on the lateral malleolus and on the head of the radius. For patients this was done at the side which displayed the most severe tremor (13 right, 6 left). The side of recording in control subjects was matched to the patients (14 right, 7 left).

Offline MR artefact correction followed the method described earlier (Allen *et al.,* 2000; van *et al.,* 2005), including low-pass filtering (400 Hz), and down-sampling (1000 Hz). Subsequently, we applied high-pass filtering (25 Hz, to remove possible movement artefacts) and rectification. We used the EMG recordings from the leg muscle to control for overt leg muscle movements. We considered the root mean square (rms) of the EMG signals measured during the imagery time (imagery epoch) and during the ITI (inter trial epoch) for each trial of the imagery experiment. For each subject, the average rms value of the EMG measured during the imagery time epoch was

normalized to the average rms value of the ITI epoch, testing for an effect of GROUP (PD, controls) and TASK (MI, VI) with a repeated measures ANOVA.

We used the EMG recording of the forearm muscle to correct for tremor related cerebral activity in the fMRI data. First, the whole EMG time series was segmented (one segment for each EPI volume). Subsequently a time frequency analysis was performed. That is, we calculated (for each segment) EMG power between 0 – 20 Hz. The peak frequency between 4 and 6 Hz. (i.e. the frequency corresponding to the rest tremor) was determined for each individual subject after visual inspection of the average power spectrum. Subsequently, the EMG power at this frequency was extracted in Matlab (MathWorks, Natick, MA) using the FieldTrip toolbox for EEG/MEG analysis (www.ru.nl/neuroimaging/fieldtrip). We also calculated the EMG amplitude and we log-transformed the EMG power to minimize outliers, leading to three tremor-related EMG regressors (power, amplitude and log of power). Last, we applied a z-transformation to each of these three regressors and convolved them with the hemodynamic response function (hrf), before adding them to our statistical model.

5. Preprocessing of imaging data

Functional data were pre-processed and analyzed with SPM5 (Statistical Parametric Mapping, www.fil.ion.ucl.ac.uk/spm). The first four volumes of each patient's data set were discarded to allow for T1 equilibration. The remaining functional volumes were spatially realigned using a least squares approach and a 6 parameter (rigid body) spatial transformation (Friston *et al.,* 1995). Subsequently, the time-series for each voxel was temporally realigned to the acquisition of the first slice. Images were normalized to a standard EPI template centered in MNI (Montreal Neurological Institute) space (Ashburner and Friston, 1997) and resampled at an isotropic voxel size of 2 mm. The normalized images were smoothed with an isotropic 10 mm full-width-at-half-maximum Gaussian kernel.

Anatomical images were spatially coregistered to the mean of the functional images (Ashburner and Friston, 1997), spatially normalized by using the same transformation matrix applied to the functional images and finally segmented into grey matter, white matter, CSF and other nonbrain partitions (Ashburner and Friston, 2005).

6. First level statistical analysis of imaging data

The ensuing pre-processed fMRI time series were analyzed on a subject-by-subject basis using an event-related approach in the context of the General Linear Model (Friston *et al.,* 1995). The model was aimed at finding regions in which the cerebral response changed as a function of TASK (MI, VI) and/or PATH WIDTH. PATH LENGTH was also considered in the analysis, which gave rise to a model with twenty different regressors of interest. The model also included separate regressors of no interest, modelling BOLD activity evoked by picture inspection, button presses, and incorrect trials, separately for each session. Each effect was modelled on a trial by trial basis as a concatenation of square-wave functions convolved with a canonical haemodynamic response function, down sampled at each scan, generating a total of 26 task-related regressors (Friston *et al.,* 1998). For the regressors of interest, onsets of the square-wave functions were time-locked to the button press marking the onset of imagery, and durations corresponded to the imagery time of each separate trial (eg. time between the two button presses). For the picture inspection regressors, onsets were time locked to the onset of picture presentation, and offsets were time-locked to the button press marking the onset of imagery. For the button press regressor, onsets were time locked to the button press marking the offset of imagery, and duration was set to zero. For the incorrect trials regressor, onsets were time locked to the onset of picture presentation, and offsets were time-locked to the button press marking the offset of imagery. The potential confounding effects of residual head movement-related effects were modelled using the time series of the estimated head movements during scanning. We included the original time series, the squared, the first-order derivatives of the originals and the first-order

derivatives of the squared (Lund *et al.,* 2005). The intensity changes attributable to the tremor-related movements through the magnetic field were accounted for by using the time series of the mean signal from the white matter, cerebral spinal fluid and out of brain voxels (Verhagen *et al.,* 2006). Finally, the three EMG regressors of the arm muscle (power, amplitude and log transformation of the power) were modelled (Helmich *et al.,* 2010), and the data was high-pass filtered (cut-off 128 s) to remove low-frequency confounds such as scanner drifts.

7. Details on region of interest analysis

Besides the whole brain analysis, statistical inference was also performed on regions of interest that were based on our previous study in healthy controls (Bakker *et al.,* 2008). More precisely, we considered the maximum coordinates of the clusters that were previously found to be significantly activated in the following contrasts: 1) MI>VI; and 2) MI-narrow>MI-broad, masked with (MI-narrow>MI-broad) > (VI-narrow>VI-broad).

This concerned the following coordinates [x y z]:

1) MI>VI:
   - i. Superior frontal gyrus left: [-12 -10 68]
   - ii. Superior frontal gyrus right; [16 -12 74]
   - iii. Anterior cingulated gyrus: [6 0 46]
   - iv. Superior parietal lobule left [-16 -58 60]
   - v. Superior parietal lobule right [20 -56 68]
   - vi. Putamen [-24 -4 8]
2) MI-narrow>MI-broad
   - i. Superior parietal lobule left [-16 -50 64]
   - ii. Superior parietal lobule right [16 -54 64]
   - iii. Middle occipital gyrus [56 -70 -12]

The set of coordinates obtained from contrast 1) were used for the analyses considering the effects of TASK and GROUP, the set of coordinates obtained from contrast 2) were used for the analyses considering the effects of PATH WIDTH and GROUP. More specifically, we drew spherical ROIs centred at these coordinates with a radius of 8 mm, using WFU Pickatlas. Statistical inference was performed at the voxel level, with a family-wise error correction for multiple comparisons ($p < 0.05$).

8. Details on a post-hoc analysis assessing the cerebral effects evoked during MI of walking

Whole-brain and ROI analyses on differential imagery-related effects did not activate parts of the known locomotor network (Jahn *et al.*, 2004; la Fougere *et al.*, 2010), in either patients or controls. However, the locomotor network was not defined using a comparison between motor imagery of walking and imagery of object motion, as done in this study. Accordingly, we performed a new analysis more closely matched to that used in the studies defining the locomotor network (Jahn *et al.*, 2004; la Fougere *et al.*, 2010). More precisely, in order to better approximate the comparison between imagining to walk and imagining to lie in a horizontal position (as used in previous papers defining the locomotor network (Jahn *et al.*, 2004; la Fougere *et al.*, 2010), we considered the cerebral effects evoked during motor imagery of walking as compared to the inter-trial epochs. Whole-brain statistical inference was based on the same threshold used in the rest of the study (FWE 0.05 cluster-level, on the basis of a >3.4 intensity). When using this approach we could clearly observe significant cerebellar and striatal activity in both controls and patients (see Supplementary Table 2, Figure 2).

9. Details on voxel-based morphometry

Voxel-based morphometry (VBM) analyses were done in SPM8. We segmented the anatomical MRI scan of each subject into grey matter, white matter, cerebrospinal fluid (CSF), and extra-cerebral compartments (e.g. out-of-brain, skull, skin). We used the DARTEL toolbox (Ashburner, 2007) to create a group-specific anatomical template and register all individual images to this template. All images were subsequently normalized to MNI space, while correcting for volume changes induced by normalization (ie. modulation). Last, we smoothed all images using a kernel of 8 mm FWHM.

Global (differences) in grey matter volume and white matter volume were quantified by integrating the tissue probabilities over all voxels. In order to avoid possible edge effects around the border between grey and white matter, we used an absolute grey and white matter threshold of $P < 0.15$.

Global differences in volume between groups were assessed using a two-tailed multivariate linear regression analysis that considered age as a covariate. Regional (i.e. voxel-by-voxel) differences in volume between groups were assessed with t-tests using the general linear model. We considered age and gender as confounding covariates in addition to total grey matter, white matter or CSF volume for the different test respectively (Good *et al.,* 2001; Pell *et al.,* 2008). The results were corrected for search volume by using family-wise error (FWE) correction ($p < 0.05$). We also considered the fMRI cluster in the mesencephalic locomotor region (MLR, see main results and Table 4) as a region of interests for additional analysis.

Supplementary Table 1. Stereotactic coordinates of the local maxima showing cerebral activity during motor imagery of gait for each group

Contrast	*Anatomical label*	*Cluster size*	*Hemi-sphere*	*Z-value*	*p-value*	*x*	*y*	*z*
cMI>cVI	Superior frontal gyrus	236	L	4.0	0.001	-8	-16	70
	Superior frontal gyrus	83	R	3.5	0.006	10	-16	72
	Superior parietal lobule	163	L	3.7	0.003	-10	-56	64
	Superior parietal lobule	159	R	4.3	< 0.001	12	-56	68
	Anterior cingulate gyrus	175	R	3.4	0.008	4	-4	40
	Putamen	193	L	3.0	0.023	-16	-4	8
pMI>pVI	Superior frontal gyrus	184	R	3.3	0.011	12	-18	74
nfMI>nfVI	Superior frontal gyrus	241	R	3.6	0.005	10	-16	72
	Superior frontal gyrus	150	L	3.5	0.005	-8	-16	68
fMI>fVI *	Posterior mid-mesencephalon	330	R	5.2	0.004	2	-30	-18

The results are based on ROIs coordinates derived from {Bakker Helmich 2008, using voxel-level family-wise inference ($p<0.05$).

* This result is based on whole-brain analysis, using cluster-level family-wise inference.

Stereotactic coordinates are reported in Montreal Neurological Institute (MNI) space.

c = controls; p = patients; nf = non-freezers; f = freezers; MI = motor imagery; VI = visual imagery; R = right; L = left;

Supplementary Table 2. Stereotactic coordinates of the local maxima showing cerebral activity during motor imagery of gait *versus* baseline for controls and patients

Contrast	*Anatomical label*	*Cluster size*	*Hemi-sphere*	*Z-value*	*p-value*	*x*	*y*	*z*
cMI > baseline	Superior frontal gyrus	6982	L	Inf	<0.001	0	0	60
			L	7.74		-24	-8	54
			R	7.04		30	-6	60
	Inferior parietal lobule	5301	L	Inf	<0.001	-12	-70	60
			L	7.51		-44	-46	54
			L	7.25		-50	-38	50
	Supra marginal gyrus	1306	R	7.81	<0.001	48	-36	44
			R	3.36		58	-42	40
	Inferior frontal gyrus	2333	L	7.68	<0.001	-52	10	2
			L	5.99		-52	6	34
	Putamen		L	5.82	<0.001	-28	18	8
	Inferior frontal gyrus	1927	R	6.62	<0.001	54	10	10
			R	6.38		58	10	20
			R	5.55		30	22	6
	Cerebellum (VI, Cr1)	1177	R	6.31	<0.001	34	-54	-32
			R	5.84		46	-60	-30
			R	5.85		34	-50	-30
	Middle frontal gyrus	591	L	6.29	<0.001	-36	36	32
	Middle frontal gyrus	220	R	4.90	0.029	38	40	32
	Cerebellum (VI, Cr1)	232	L	4.65	0.024	-34	-54	-34
pMI > baseline	Superior frontal gyrus	27984	L	Inf	<0.001	-2	4	58
			R	Inf		4	-2	66
			L	Inf		-4	-4	68
	Cerebellum (V1, Cr1, VIIIA)	1097	L	6.57	<0.001	-48	-60	-28
			L	4.57		-34	-56	-34
			L	4.32		-36	-50	-50
	Cerebellum (VI, CR1, VIIIA)	1098	R	5.14	<0.001	44	-62	-30
			R	5.08		32	-60	-30
			R	4.96		32	-34	-50

The results are based on whole-brain analysis, using cluster-level family-wise inference ($p<0.05$). Stereotactic coordinates are reported in Montreal Neurological Institute (MNI) space.

c = controls; p = patients; MI = motor imagery; R = right; L = left;

Supplementary Figure 1. Average tissue type volume within MLR

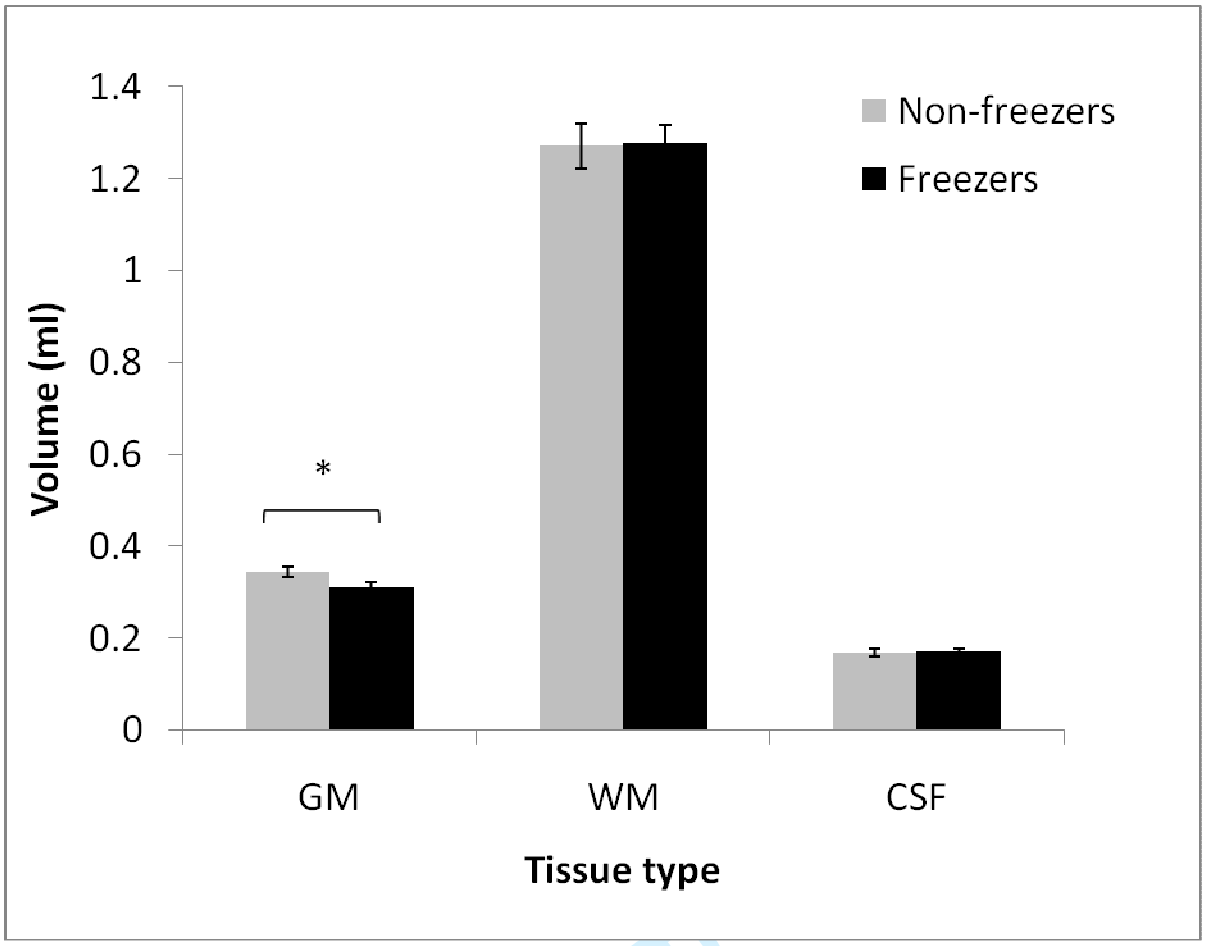

Suppl. Figure 1. Average volume (± SEM) of different tissue classes within the MLR activation blob, determined for freezers and non-freezers.

Supplementary Figure 2. Motor imagery related brain activity

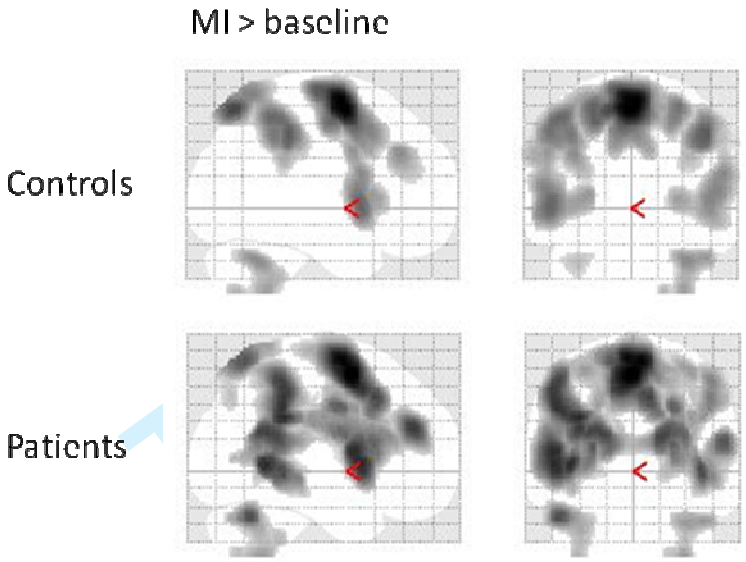

Suppl. Figure 2. SPM{t} maps of increase in activity for motor imagery (MI) versus baseline for patients and controls separately. The results are based on whole-brain analysis, using cluster-level family-wise inference ($p<0.05$).

Reference List

Allen PJ, Josephs O, Turner R. A method for removing imaging artifact from continuous EEG recorded during functional MRI. Neuroimage 2000; 12: 230-239.

Ashburner J. A fast diffeomorphic image registration algorithm. Neuroimage 2007; 38: 95-113.

Ashburner J, Friston K. Multimodal image coregistration and partitioning--a unified framework. Neuroimage 1997; 6: 209-217.

Ashburner J, Friston KJ. Unified segmentation. Neuroimage 2005; 26: 839-851.

Bakker M, de Lange FP, Helmich RC, Scheeringa R, Bloem BR, Toni I. Cerebral correlates of motor imagery of normal and precision gait. Neuroimage 2008; 41: 998-1010.

Friston KJ, Fletcher P, Josephs O, Holmes A, Rugg MD, Turner R. Event-related fMRI: characterizing differential responses. Neuroimage 1998; 7: 30-40.

Friston KJ, Holmes AP, Poline JB, Grasby PJ, Williams SC, Frackowiak RS*, et al*. Analysis of fMRI time-series revisited. Neuroimage 1995; 2: 45-53.

Good CD, Johnsrude IS, Ashburner J, Henson RN, Friston KJ, Frackowiak RS. A voxel-based morphometric study of ageing in 465 normal adult human brains. Neuroimage 2001; 14: 21-36.

Helmich RC, Derikx LC, Bakker M, Scheeringa R, Bloem BR, Toni I. Spatial Remapping of Cortico-striatal Connectivity in Parkinson's Disease. Cereb Cortex 2010.

Jahn K, Deutschlander A, Stephan T, Strupp M, Wiesmann M, Brandt T. Brain activation patterns during imagined stance and locomotion in functional magnetic resonance imaging. Neuroimage 2004; 22: 1722-1731.

la Fougere C, Zwergal A, Rominger A, Forster S, Fesl G, Dieterich M*, et al*. Real versus imagined locomotion: a [18F]-FDG PET-fMRI comparison. Neuroimage 2010; 50: 1589-1598.

Lund TE, Norgaard MD, Rostrup E, Rowe JB, Paulson OB. Motion or activity: their role in intra- and inter-subject variation in fMRI. Neuroimage 2005; 26: 960-964.

Pell GS, Briellmann RS, Chan CH, Pardoe H, Abbott DF, Jackson GD. Selection of the control group for VBM analysis: influence of covariates, matching and sample size. Neuroimage 2008; 41: 1324-1335.

van DH, Zijdewind I, Hoogduin H, Maurits N. Surface EMG measurements during fMRI at 3T: accurate EMG recordings after artifact correction. Neuroimage 2005; 27: 240-246.

Verhagen L, Grol MJ, Dijkerman HC, Toni I. Studying visually-guided reach to grasp movements in an MR-environment. Neuroimage 2006; 31: S45.